

Analysis of the ZPR-9 gas-cooled fast reactor experiments using JEF-2.2 data and the ERANOS code system

Jean Tommasi^{*1}

¹DER/SPRC, building 230, CEA-Cadarache, 13108 Saint Paul lez Durance CEDEX, France

The recent renewal of interest for gas-cooled fast reactors has led CEA to revisit past experiments for code validation purposes. Several configurations of the first phase of the gas-cooled fast reactor experiments performed in 1975-76 in the Zero Power Reactor 9 critical facility at Argonne National Laboratory have been reanalyzed using the ERANOS-2.0 neutronics code system and JEF2-based unadjusted and adjusted nuclear data libraries. Some numerical validations have been performed with the Monte-Carlo code TRIPOLI-4. The reactivity scale (delayed neutron fraction, inhour value) is predicted within the experimental uncertainty. The criticality of the core is correctly predicted (discrepancy <0.5%) even if the calculated magnitude of the heterogeneity and streaming effects, although small, differs significantly between the deterministic (-0.46%) and stochastic (-0.22±0.03%) calculations. Fission spectral indices relative to Pu239 are well predicted (discrepancy <2%), but capture indices are underestimated by ≈8 %.

KEYWORDS: *gas-cooled fast reactors, critical experiments, ZPR-9, code validation, ERANOS*

1. Introduction

Innovative gas-cooled fast reactor (GCFR) concepts have specific features that distinguish them markedly from standard Na-cooled fast reactors. As an illustration, we show below a comparison of the main features of prospective GCFR designs now being studied at CEA with respect to conventional Na-cooled fast reactors.

Standard Na-cooled fast reactors

- Na cooling
- Oxide fuel (sintered pellets)
- No matrix
- Steel cladding
- Fertile blanket or steel reflector

Innovative gas-cooled fast reactors

- He cooling (high temperature)
- Carbide fuel (particles): denser to improve breeding ratio in fuel
- Inert matrix (SiC)
- Innovative, heat resistant structures (SiC)
- Innovative, heat resistant reflector (Zr_3Si_2 , ZrC or SiC)

The expected consequences of such differences on neutron physics parameters include:

- Na void effect (several \$) replaced by He depressurization effect which may nevertheless exceed 1\$ due to large He pressure
- Neutron streaming through the He-filled channels

* Corresponding author, Tel. +33 4 42 25 75 66, FAX +33 4 42 25 70 09, E-mail: jean.tommasi@cea.fr

- Softer neutron spectrum than in a standard fast reactor (large amounts of carbon)
- Increased impact of less well known nuclear data (higher Pu data, Si, Zr, ...)

It is important to establish whether current neutronics code systems and associated data can be validly used for computing such innovative systems and to what extent additional developments, experiments and benchmarking may be required. To this aim, it was decided to analyze existing GCFR experiments with the ERANOS [1] code system developed for conventional Na-cooled fast reactors. Among the selected experiments are the GCFR series of cores performed over the 1975-76 period in the Zero Power Reactor-9 (ZPR-9) facility at Argonne National Laboratory (ANL), USA. They were designed to provide a reference set of reactor physics measurements in support of the 300 MWe GCFR Demonstration Plant designed at the time by General Atomic Company.

These experiments were divided in three phases. The Phase I experiments cover mainly a thorough characterization of the core criticality and kinetics parameters, as well as Pu ageing and temperature coefficients. Phase II involves a Doppler effect measurement (small heated sample at the core center), a He depressurization experiment (small cylinder in the central core drawer) and a simulation of a full core steam ingress (polyethylene foam loaded in all fuel drawers). Finally, Phase III includes a large pin zone at the core center (pin-type vs. platelet-type streaming).

The Phase I experiments have been analyzed at CEA-Cadarache, and the main results are summarized below.

2. Data and code systems used for the analysis

The ERANOS code system is used for deterministic calculations [1]. The latest release is ERANOS-2.0. The nuclear data libraries used by ERANOS are derived from the JEF-2.2 nuclear data evaluated file [2] by using the processing codes NJOY and CALENDF [3]. They include a fine group library (1968 energy groups) containing 37 nuclides (U and Pu isotopes, main coolant and structural materials), and three broad group libraries (175 groups for shielding applications, 172 groups for thermal spectrum applications, and 33 groups for fast spectrum applications) containing approximately 350 nuclides each. A statistical adjustment, based on a generalized least squares method, has been performed on the JEF-2.2 libraries, using over 350 integral experiment values, to produce the adjusted ERALIB-1 libraries [4].

ERANOS includes the cell code ECCO [5] based on collision probabilities routines to model complex geometries and on the subgroup method for accurate resonance self-shielding assessment. ECCO provides the smeared and condensed (33 groups) cross-section data to be used by the reactor flux solvers. In the ECCO code the neutron balance of the cell is preserved by condensation and smearing.

In this work, the BISTRO 2D finite-difference Sn transport module has been used [6], involving P1 scattering law and S8 angular description, with a mesh size of about 5 cm, radially and axially in a RZ cylindrical geometry (we have checked that the mesh effect on reactivity is then negligible).

Some results have been checked against a Monte-Carlo code, TRIPOLI-4 [7], using a continuous energy library based on JEF-2.2 data consistent with the libraries used in ERANOS, in order to provide a numerical validation of the ERANOS calculation scheme.

3. A brief description of the GCFR phase I experiments in the ZPR-9 critical facility

A detailed and comprehensive description and discussion of the geometry, loading, and results of the GCFR Phase I experiments is available in a single report by ANL [8]. In the ZPR-9 facility, basic materials are manufactured as plates, loaded vertically into drawers (see Fig. 2); the drawers are then loaded horizontally in the stationary half and moveable half of the assembly.

The basic features of the GCFR-I assembly were designed to be representative of general GCFR design characteristics. The core is a homogeneous single-zone almost cylindrical region with horizontal axis (the Z axis), surrounded by axial and radial blankets. The fuel is made of a mixture of UPuMo platelets (with high-grade plutonium), U_3O_8 platelets and Fe_2O_3 platelets in order to simulate oxide fuel with steel cladding. Air-filled (“void”) platelets are added to simulate the gas channels. The resulting gas volume fraction is 53%. Radial and axial blanket unit cells are built from U_3O_8 , depleted U and void platelets. The fissile height is 122 cm and the fissile equivalent diameter 180 cm. The axial blanket thickness is 30 cm, and the radial blanket equivalent thickness 25 cm. Figure 1 shows a cross-cut of the assembly at core mid-plane. It is a sketch of the stationary half of the core, depicting the as-built configuration. Because of fuel platelet length limitations in the fuel inventory, the whole core could not be assembled with identical fuel platelet-length loadings, and three loadings with slightly different fuel platelet-length combinations have been identified as Zone 1, 2 and 3 in the figure.

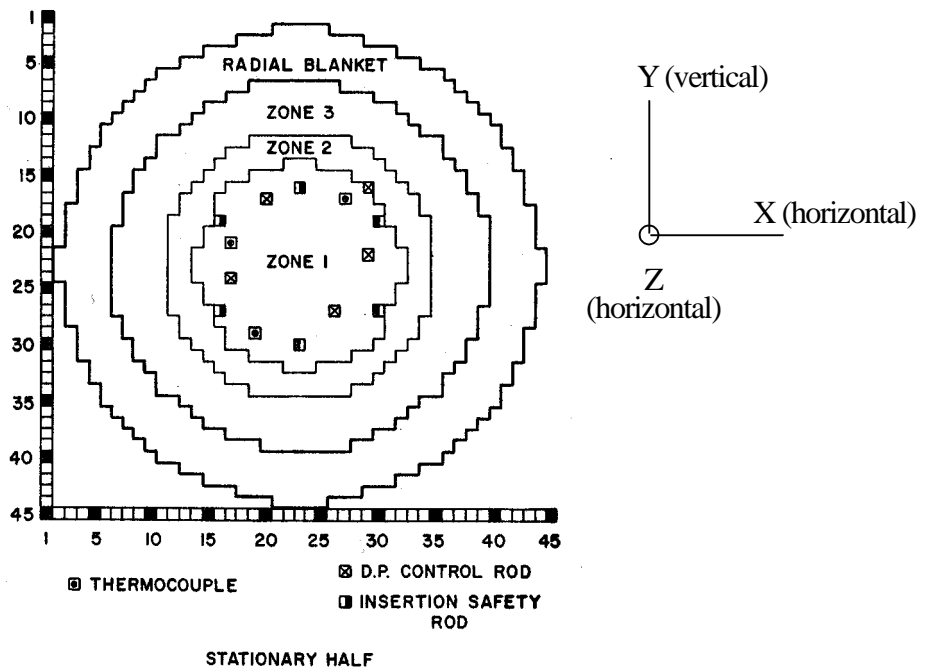


Fig. 1 X-Y view of the stationary half of the GCFR-I assembly showing the as-built configuration (this is a copy of Fig. 4 in Reference [8])

The typical cell structures for fuel, radial and axial blanket are given in figure 2.

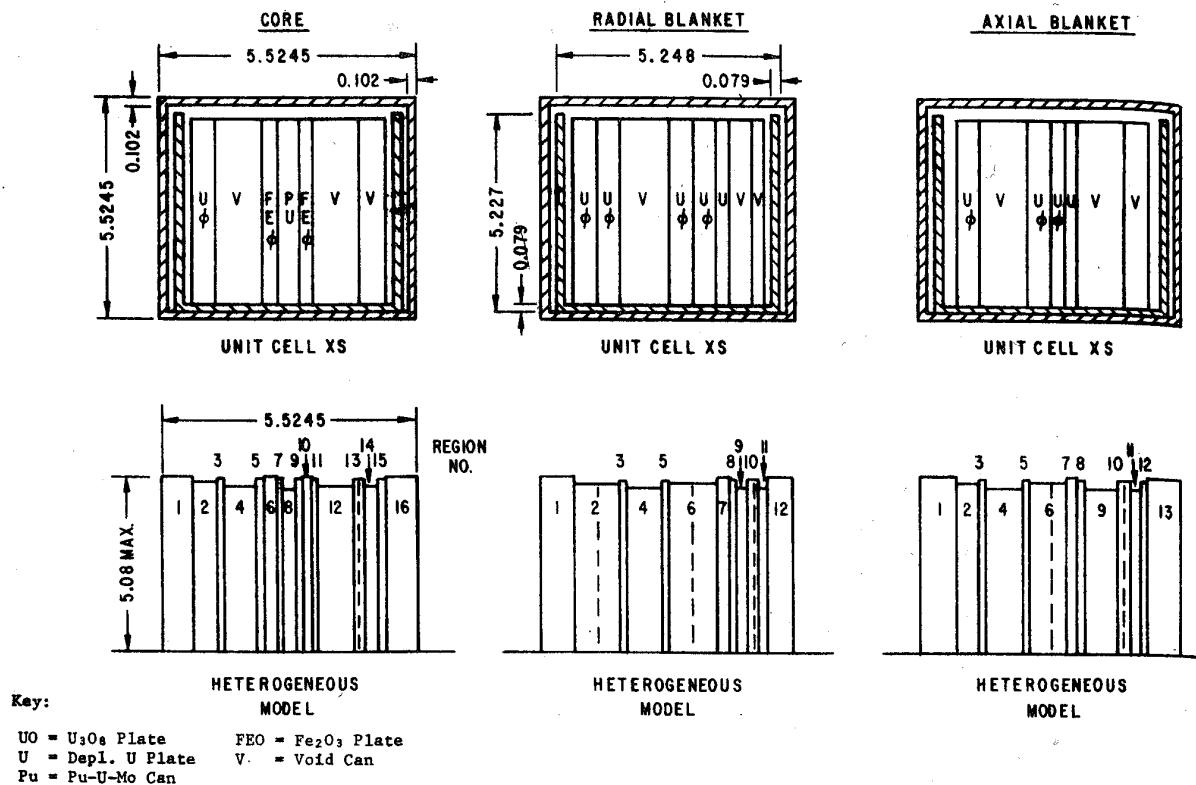


Fig. 2 Unit cell structures (actual and model). All dimensions in cm (this is a copy of Fig. 1 in Reference [8])

A list of the measurements performed in the Phase I experiments is given below.

1. Approach-to-critical, critical mass
2. Neutron spectra at core center (proton-recoil technique)
3. Spectral indices at core center (fission counters and foil irradiations)
4. Sample reactivity worth (sample oscillation reactivity difference technique)
5. Radial and axial fission rate profiles (foil irradiations)
6. Kinetics parameters (rod-drop die-away flux profile technique) and β_{eff} (detector-variance method)
7. Octant with checkerboard loading (figure 3): reactivity change, radial reaction rate traverses
8. Reactivity worth of steam entry in central core zone (simulated with polyethylene foam strips)

Items 2, 4 and 8 will not be addressed in this analysis. For item 7, the checkerboard loading of platelets was performed in a quadrant of the stationary half of the assembly, where alternate drawers were loaded with horizontal (instead of vertical) platelets. This was meant to cut off the streaming channels: in the normal drawer loading (all plates vertical), streaming channels exist in the Y and Z directions while in the checkerboard loading, direct streaming channels exist only in the Z direction.

4. Results of the analysis

4.1 Calculation scheme

Fuel and blanket cells have been modeled by ECCO in a plane (1D) heterogeneous geometry, with reflection boundary conditions. Fuel cell calculations involve a broad group step (heterogeneous geometry) with a buckling search in order to make the cell critical, followed by a fine group step (heterogeneous geometry as well). Then the cross-sections are smeared and condensed to 33 energy groups. The blanket cells, being subcritical, are fed by an external neutron source taken as the fuel cell flux times the core diffusion coefficient. A treatment of heterogeneity and streaming effects can be achieved in ECCO by using a 2-D exact representation of fuel subassemblies combined with the directional Benoist formulation, to produce equivalent homogeneous cross sections for use in whole core calculations [9]. In order to check the value of heterogeneity and streaming effects, homogeneous cell calculations have also been run.

The whole core calculations are performed in RZ geometry, with 33 energy groups, using either the ERANOS modules for the diffusion approximation (with directional diffusion coefficients) or Sn transport.

A numerical validation has been provided by running the Monte-Carlo code TRIPOLI-4 on two RZ geometries : one with a homogeneous description of fuel and blanket zones, the other with a 1D plane description in the fuel and blanket zones corresponding to the description in ECCO. In the latter case, this means that the exact drawer/platelet geometry has not been represented, but rather an idealization meant to be as close as possible to the ECCO description, in order to check the validity of the ECCO built-in procedure to treat heterogeneity and streaming effects. Previous checks against Monte-Carlo subassembly calculations showed a good agreement [9].

4.2 Kinetics parameters and reactivity effects

The kinetics parameters investigated here include the delayed neutron fraction (β_{eff}), the averaged delayed neutron lifetime (τ_{del}), and the inhour, which is the reactivity unit used in the report [8]. Note that throughout this analysis, the inhour value used has been the one computed by ERANOS. The prompt neutron lifetime (Λ) computed by ERANOS is 0.459 μs , and may be compared to the value computed by ANL in 1976 : 0.447 μs (difference of less than 3%).

The reactivity worth of Pu241 was experimentally determined by measuring the reactivity excess of the reference configuration at different times over a period of 62 days during the experimental program, with a rather important experimental uncertainty of $\approx 13\%$. The central drawer worth was measured relative to void in that location.

Table 1 shows the ratio of calculation to experiment ratios (C/E) for the above parameters. The uncertainty quoted is the experimental standard deviation provided in Ref. [8]. The C/E values are satisfactory, differing from unity by less than two experimental standard deviations.

Table 1 GCFR-I kinetics parameters and reactivity effects : comparison to experiment

Parameter	C/E
Delayed neutron fraction (β_{eff})	0.963 ± 0.023
Averaged delayed neutron lifetime (τ_{del})	1.011 ± 0.018
Inhour	0.973 ± 0.030
Pu241 ageing	0.934 ± 0.123
Central drawer reactivity worth	1.014 ± 0.018

4.3 Core criticality and reaction rate distributions

Table 2 provides the calculated multiplication factors, according to code (ERANOS or TRIPOLI), cell model (homogeneous or heterogeneous) and data library (unadjusted or adjusted), including model biases. The statistical uncertainties on the multiplication factor are given in Table 3 ; the statistical uncertainty on Monte-Carlo predictions is quite small ($\delta k = \pm 0.00021$) due to the large number of neutron histories taken into account (2000 batches of 10000 histories each). Finally, Table 4 yields the best estimate values and associated uncertainties.

Table 2 Calculated multiplication factors and biases

	ERANOS-2.0	TRIPOLI-4
Homogeneous cells, JEF-2.2 data	0.99478	0.99515
<i>Bias 1 : heterogeneity + streaming</i>	-0.00461	-0.00217
Heterogeneous cells, JEF-2.2 data	0.99017	0.99298
<i>Bias 2 : neutron reflection on outside structures</i>	+0.00310	
<i>Bias 3 : Pu239 mass scaling</i>	+0.00200	
Heterogeneous cells, JEF-2.2 data, best estimate	0.99527	0.99808
<i>Bias 4 : data adjustment</i>	+0.00631	
Heterogeneous cells, ERALIB-1 data, best estimate	1.00158	(1.00439)

Bias 1 is simply the difference between the multiplication factors of the heterogeneous and homogeneous models, resulting from heterogeneity and streaming effects. The Monte Carlo prediction ($\delta k = -0.00217 \pm 0.00030$) differs significantly from the value calculated by the deterministic code system ($\delta k = -0.00461$). The latter includes a predominant heterogeneity effect ($\delta k = -0.00387$) and a smaller “streaming” effect due to the use of directional diffusion coefficients (for diffusion calculations) instead of an average diffusion coefficient ($\delta k = -0.00074$). This discrepancy should be investigated further, even though the global effect is quite low (less than 0.5%).

Bias 2 is introduced because the calculations model only the core and blankets with a void condition at the outer blanket boundary, whereas the core structure supports (bed, knees) and other materials (e.g. void drawers) around the assembly actually reflect some of the exiting neutrons back to the assembly. This effect has been estimated by ANL [8], and their suggested corrective bias is used here.

Bias 3 is motivated by the slight discrepancy between the mass Pu239 inventory of the core built using the compositions of the report and the actual loaded fissile mass record [8].

Bias 4 is simply the difference between ERANOS calculations using either the adjusted ERALIB-1 libraries or the unadjusted JEF-2.2 libraries.

Table 3 Relative uncertainties (1 standard deviation) on multiplication factors

	Uncertainty
Statistical uncertainty on Monte-Carlo results	± 0.00021
Nuclear data (JEF-2.2 library covariance matrix)	± 0.01710
Nuclear data (ERALIB-1 library covariance matrix)	± 0.00129
Loaded critical mass	± 0.00300

The uncertainty due to the loaded critical mass is the translation in terms of reactivity of the Pu239 mass uncertainty quoted in the loaded fissile mass record [8]. The uncertainties due to nuclear data have been computed using the k_{eff} sensitivity vectors (by nuclide, reaction and energy group) of the assembly and the covariance matrices associated to the JEF-2.2 and ERALIB-1 libraries respectively.

Table 4 Calculated multiplication factors : best estimates with uncertainties (1 standard deviation)

Nuclear data library	ERANOS-2.0	TRIPOLI-4
JEF-2.2 (unadjusted)	0.99527 ± 0.01728	0.99808 ± 0.01733
ERALIB-1 (adjusted)	1.00158 ± 0.00327	(1.00439 ± 0.00329)

The measured value is $k = 1.00081 \pm 0.00003$. As a global result, the criticality prediction with ERANOS or TRIPOLI is good: discrepancies are less than 0.5%.

The measured effect of the checkerboard loading on reactivity was quite small ($+23 \pm 4$ inhour, i.e. $+0.025 \pm 0.004\%$). The calculation options used in the ERANOS calculations, i.e. a plane (1D) unit cell geometry and the use of directional diffusion coefficients that are linear combinations of the diffusion coefficients in directions parallel and orthogonal to the plates, make it almost meaningless to check them precisely against such a small experimental value. As a matter of fact, the use of directional instead of cell-averaged diffusion coefficients (computed with a plane 1D unit cell geometry) induced a reactivity change of only 0.07% at the full core level, as seen above (discussion on bias 1).

4.4 Spectral indices and reaction rate distributions

The following indices, relative to Pu239 fission, have been measured: U233, U235, U238, Pu240, Th232 (fission), and U238, Th232 (capture). Calculation to experiment ratios are presented in Table 5 below. The uncertainties quoted are the experimental uncertainties (1 standard deviation) taken from the report [8]. For lack of detailed information, the corrective factors for taking into account detector detailed structure have been applied using the values recommended by ANL [8].

Table 5 Spectrum indices at core center: comparison to experiment

Spectral index	C/E (JEF-2.2 data)	C/E (ERALIB-1 data)
F(U233) / F(Pu239)	1.010 ± 0.018	0.999 ± 0.018
F(U235) / F(Pu239)	1.002 ± 0.012	0.984 ± 0.012
F(U238) / F(Pu239)	1.026 ± 0.012	0.992 ± 0.012
C(U238) / F(Pu239)	0.932 ± 0.011	0.922 ± 0.011
F(Pu240) / F(Pu239)	1.089 ± 0.012	1.054 ± 0.012
F(Th232) / F(Pu239)	1.036 ± 0.071	1.016 ± 0.071
C(Th232) / F(Pu239)	0.944 ± 0.011	0.928 ± 0.011

The prediction of spectral indices at the core center is good for U233, U235 and U238 (fission) but poor for the threshold-based fission indices of Th232 and especially Pu240 (overestimated) and the capture indices Th232 and U238 (underestimated). Using adjusted data results in no significant improvement except for Pu240 fission; the capture indices even worsen a little when using adjusted data.

The discrepancy in the U238 capture index is particularly puzzling, due to the large sensitivity of the multiplication factor to the capture of U238: such a large (7 to 8%) underestimation of the C(U238)/F(Pu239) ratio is inconsistent with the quality of the criticality prediction (<0.5%), and of the U233, U235 and U238 fission indices. The detectors used for spectral index measurement were fission flow counters for fission rates and foil irradiations for capture rates [8]. It is believed that a better description of the detailed structure and position of these foils could help in reducing the discrepancy.

Axial reaction rate distributions (normalized to 1 at the core mid-plane) for U235 (fission), U238 (fission and capture) and Pu239 (fission) show a close agreement with experimental data in the core (underestimation by less than 3%), but in the axial blanket the gradient is overestimated by the calculation. This is consistent with the void condition taken at the outer boundary of the blankets, whereas there are some structures reflecting neutrons outside the blankets: this was the reason for the +0.00310 correction on k_{eff} quoted in Table 2.

5. Conclusion

The GCFR Phase I series of experiments has been analyzed with the ERANOS code system and JEF2-based nuclear data. These experiments are partly representative of a fast system without sodium and with “void” regions, i.e. a gas-cooled fast reactor.

The reactivity scale is well predicted (delayed neutron fraction and average lifetime, inhour value), as the calculated results fall within the experimental uncertainty.

The prediction of core criticality is reasonably accurate (discrepancy <0.5% when all model biases have been taken into account). However, a discrepancy still remains in the amplitude of heterogeneity and streaming effects between the deterministic code system ERANOS (-0.46%) and the Monte-Carlo code TRIPOLI-4 (-0.22±0.03%), even if the size of this discrepancy remains within the experimental and calculation uncertainties (±0.33% at best). The reasons for this discrepancy should be investigated further.

The prediction of spectral indices relative to Pu239 fission is good for fission indices: U233, U235, U238, Th232 (discrepancy less than 2% using adjusted data) with the exception of Pu240 (overestimation of 9% with unadjusted data, reduced to 5% with adjusted data). The prediction of capture indices (U238 and Th232) remains poor with an underestimation by 7 to 8%. This is inconsistent with the reactivity prediction. Further investigations have to be performed on the detailed structure and positions of the foil detectors used for the capture index measurement.

Some experiments of the GCFR Phase II and III series will be analyzed in 2004, namely the steam entry simulation with polyethylene foam strips at full core scale and the reactivity weight of helium among the Phase II experiments, and the configuration with a 60 cm diameter pin zone at core center among the Phase III experiments.

Acknowledgement

All data relative to the GCFR critical assemblies have been provided by Argonne National Laboratory in the framework of a CEA-DOE cooperation agreement in the field of advanced nuclear reactors.

References

- 1) G. Rimpault et al., "The ERANOS code and data system for fast reactor neutronic analysis", Proc. Int. Conf. on the new frontiers of nuclear technology : reactor physics, safety and high-performance computing, PHYSOR'2002, Seoul, Korea, Oct. 7-10, 2002
- 2) "The JEF-2.2 nuclear data library", JEF report 17, OECD/NEA, April 2000
- 3) C.J. Dean et al., "Production of fine group data for the ECCO code", Proc. Int. Conf. on the physics of reactors: operation, design and computation, PHYSOR'90, Marseille, France, April 23-27, 1990
- 4) E. Fort et al., "Improved performances of the fast reactor calculational system ERANOS-ERALIB1 due to improved a priori nuclear data and consideration of additional specific integral data", Annals of Nuclear Energy **30**, 1879-1898 (2003)
- 5) G. Rimpault, "Algorithmic features of the ECCO cell code for treating heterogeneous fast reactor subassemblies", Proc. Int. Top. Meeting on reactor physics and computation, Portland, Oregon, May 1-5, 1995
- 6) G. Palmiotti et al., "Optimized two-dimensional Sn transport (BISTRO)", Nuclear Science and Engineering **104**, 26-33 (1990)
- 7) J.P. Both and Y. Pénéliou, "The Monte-Carlo code TRIPOLI-4 and its first benchmark interpretations", Proc. Int. Conf. on reactor physics, PHYSOR'96, Mito, Japan, Sept. 16-20, 1996
- 8) ANL internal report (1976)
- 9) G. Rimpault, P. Smith and T. Newton, "Advanced methods for treating heterogeneity and streaming effects in gas-cooled fast reactors", Proc. Int. Conf. on mathematics and computation, reactor physics and environmental analysis in nuclear applications, M&C'99, Madrid, Spain, Sept. 27-30, 1999